Revista Mexicana de Física 30 no. 1 (1983) 1-39

ON THE EFFECT OF X-IRRADIATION ON IMPURITY VACANCY DIPOLES AND THE INFLUENCE OF THEIR AGGREGATION-PRECIPITATION STATE IN THE ROOM TEMPERATURE COLORING OF THE ALKALI HALIDES †

J. Rubio O. and H. Murrieta S.

Instituto de Física, UNAM

Apartado Postal 20-364. 01000 México, D.F.

ABSTRACT

This paper presents a complete collection of the investigations which have been carried out by our group on the effects of X-irradiation in alkali halide single crystals doped with Eu^{2+}, Pb^{2+}, Ca^{2+} and Sr^{2+} ions. They were performed in order to get a better understanding of the secondary mechanism for the F-center production in these type of crystals. In particular, these studies have gathered enough experimental evidence to show that the Me^{2+} - cation vacancy dipoles act as the dominant traps for the radiation induced halogen interstitial defects. Also, it was clearly established that the X-irradiation increases considerably the rate of aggregation of dipoles.

RESUMEN

En este artículo se presentan los resultados de las investiga-

† Presentado por J. Rubio O. y H. Murrieta S. en la asamblea general ordinaria de la SMF del 15 de abril de 1983.

ciones efectuadas por nuestro grupo sobre los efectos de la irradiación, con rayos X, en cristales de halogenuros alcalinos conteniendo impurezas como Eu^{2+}, Pb^{2+}, Ca^{2+} y Sr^{2+}. Tales investigaciones fueron llevadas a cabo para obtener una mayor comprensión del mecanismo secundario de producción de centros F. En particular se ha acumulado suficiente evidencia experimental para mostrar que los complejos dipolares impureza catiónica-vacancia actúan como las trampas dominantes de los defectos intersticiales de halógeno inducidos por la radiación. Así mismo se ha establecido claramente que la irradiación incrementa considerablemente el proceso de agregación dipolar.

1. INTRODUCTION

A lot of experimental and theoretical work has been performed in order to understand the mechanisms of defect creation in the alkali halide lattices by ionizing radiation. Since the early studies, it was recognized that several types of defects were involved[1,2]. A variety of mechanisms that involve primarily the conversion of electronic excitation energy into lattice defects have been proposed in order to explain the defect creation[3,4,5] and although the general features of the process have been understood, a number of details still remain unsolved.

Up to date, the most studied defects have been the F-center and its partner the so-called H-center. At the present time there are several reviews in the literature dealing with the principal properties of these defects[6-11], and by the sake of brevity, it will be only mentioned here that it is now already clear that the radiation-induced production of F-centers involves mainly two steps:

(1) The first one consists of a primary creation event which can be postulated in terms of electron-hole overlap, which relates in turn to the separation of the F-H pair. When this pair has a significant overlap it can be treated as a self trapped exciton with a high probability of undergoing a non-radiative transition to the ground state of the crystal giving rise to a well separated F and H centers[12,13].

(2) A thermal and radiation-induced processes associated with the motion of the interstitial and vacancy centers. The subsequent trapping of the interstitials at impurities and other defects leads to the defini-

tive stabilization of the color centers after irradiation[14-17].

The production rate of stable radiation induced damage is considerably affected by the nature of the secondary reactions which take place after the primary production of F and H centers has occurred. In particular, it is well recognized that the F-center coloring curve may be divided into three stages. The first one is characterized by a rapid increase in the F-center concentration and is usually observed at low doses of irradiation. The efficiency for coloring during this stage is considerably enhanced by the presence of divalent cation impurities in the alkali halide matrix. The second stage corresponds to the saturation of the F-center growth and the third one is associated with a further steep increase in the concentration of this center, usually observed at high doses. The effect of the impurity ions on this stage is generally, to suppress it.

The enhancement at the early stage has been determined, experimentally, to be proportional to the square root of the impurity concentration[7,18-21]. This fact was interpreted in the early studies in terms of the model proposed by Crawford and Nelson[22] according to which the cation vacancies can be converted to F-centers during the irradiation processes or in terms of the model proposed by Ikeya et al.[19] in which it is assumed that the isolated cation vacancies are the fundamental traps for the mobile interstitial defects with the result of a reduction in the back reaction for the recombination of an F-center with the halogen interstitial defect. Both models predict that the transition from the first to the second stage of the F-center coloring curve would result from the exhaustion of the cation vacancies and that the amount of the first stage coloration should be proportional to the square root of impurity concentration.

Electron paramagnetic resonance (EPR) studies performed later by Hayes[23,24] lead this author to suggest that the traps for the H-centers were the vacancies associated with the impurity ions, i.e., the impurity vacancy dipoles (I-V). This suggestion was corroborated later by Hoshi and co-workers[14] through a detailed study of the absorption bands of X-irradiated calcium-doped KBr. Motivated by these results which were

in disagreement with Crawford and Nelson and Ikeya et al.'s model, Marat-Mendes and Comins[25-27] performed a series of detailed experiments in KCl:Sr^{2+} and KBr:Sr^{2} establishing that in their room temperature X-irradiated samples, there was a proportional relationship between the growth of F-centers and dipole destruction which held in both the first and second stages of the F-center growth curve. From this result these authors concluded that the isolated (I-V) dipoles appeared to be the fundamental traps for the mobile halogen interstitial defects.

On the other hand, Kao and Perlman[28] recently reported that in europium-doped KCl, the X-irradiation destroys Eu^{2+} - cation vacancy dipoles and converts the doubly valent impurity ions to a monovalent state. They also found that in the slightly doped samples, the number of dipoles destroyed by irradiation was equal to the sum of the number of converted ions and the number of F-centers produced. As before, this result suggested that the (I-V) dipoles act as the dominant traps for the radiation-induced interstitials. In the case of heavily doped samples, however, the number of dipoles destroyed exceeded the sum of the number of converted ions and the number of F-centers produced. In order to explain this result Kao and Perlman invoked the fact that the X-irradiation may increase the rate of aggregation of dipoles as it was previously suggested by Muccillo and Rolfe[29] in their study of γ-irradiated KBr:Sr^{2+}.

Recently, Aguilar et al.[30] and Comins and Carragher[31] have developed similar models in order to explain the F-center production in the alkali halides doped with divalent cation impurities. In these models it is considered that the (I-V) dipoles or dipole aggregates act as the dominant traps for the halogen interstitial atoms. According to them, the first stage of the F-center production is due to a dynamic temperature-dependent process and that the transition from the first to the second stage is not due to the exhaustion of the interstitial traps. Rather, it is the result of a dynamic saturation process where both trapping and detrapping of halogen interstitials occur. Moreover, the solution of the kinetic equations involved in the model gives an amount of first stage coloration proportional to the square root of impurity concentration, giving then a different point of view from previous models for the

origin of this relationship.

Very recently, detailed experiments have been carried out by our group on the effects of X-irradiation in alkali halides doped with several doubly valent impurities, in which the role played by the isolated dipoles as well as the impurity aggregation-precipitation state in the F-coloring efficiency have been extensively analyzed. It is the purpose of this paper to present a complete collection of these results together with those obtained by other workers.

2. EXPERIMENTAL

The alkali halide single crystals employed in these experiments were grown in our laboratory by the Czochralski technique under a controlled atmosphere of dry argon. The starting materials were always dried in vacuum for several hours to avoid contamination by OH impurities. The doubly valent impurity ions used were Ca^{2+}, Sr^{2+}, Cd^{2+}, Pb^{2+} and Eu^{2+}, and were added to the melt in different initial concentrations. The concentration of the impurities in the crystals used was determined by atomic absorption spectrophotometry. In the particular case of the europium-doped crystals, the concentration was determined through the optical absorption spectrum of the quenched samples following the procedure described elsewhere[32].

Thermal treatments were performed using conventional furnaces with a temperature control in the range of $\pm 5°C$. Quenching treatments were performed by heating the samples for $\sim$1h at 550°C and then dropping them onto a copper block at room temperature.

Optical absorption and luminescence measurements were carried out at room temperature with a Perkin Elmer model 330 double-beam recording spectrophotometer and a Perkin Elmer model 650-10S fluorescence spectrophotometer, respectively.

Irradiations were made at room temperature using X-rays from either a Philips or a Kristalloflex 2H Siemens tungsten target tubes. In both cases, the tubes were operated at 30kV and 20mA, the X-rays being filtered through a 1mm aluminium filter. Care was taken to avoid heating

of the crystals during irradiation.

In order to determine the dipole concentration in the quenched samples, ionic thermocurrent (ITC) measurements were performed with the experimental set-up described previously[33].

Finally, electron paramagnetic resonance (EPR) measurements were performed in the quenched samples in order to have a different way to the ITC, to follow the number of Eu^{2+} - cation vacancy dipoles which were destroyed during irradiation. To do that, the total concentration of impurity vacancy dipoles, as previously determined by ITC, was associated with the intensity of the fine structure groups in the EPR spectrum for the case in which the magnetic field was applied along the ⟨100⟩ direction. Then, the observed intensities of the fine structure groups after irradiation were compared to those originally observed before irradiation. Special care was taken to use the same operating conditions of the spectrometer. To perform the measurements a Varian V-4502-12 reflection type X-band spectrometer with 100 KHz field modulation and a rectangular cavity operating in the TE_{102} mode were employed. At this point, it should be pointed out that in the europium-doped crystals, the EPR technique was preferred over the ITC in order to determine the impurity-vacancy dipole destruction since measurements can be perfcrmed in shorter times preventing, therefore, the bleaching of the colored samples.

3. RESULTS AND DISCUSSION

a) *Effects of X-irradiation in NaCl*

Before irradiation, the freshly quenched europium-doped NaCl samples showed an optical absorption spectrum consisting of two broad bands whose centers of gravity peak at 240 and 347nm. These bands have been attributed to transitions from the $^8S_{7/2}$ ground state of the $4f^7$ configuration to states of the $4f^6 5d$ configuration[34]. On the other hand, the emission spectrum consists of only one band peaking at 427nm when the excitation is performed with light lying in either the high or the low energy bands of the absorption spectrum[35]. This band has been ascribed to complexes of the type Eu^{2+} - cation vacancy dipoles dispersed into the

alkali halide matrix. These complexes give rise to an ITC peak whose maximum is at 208±1K[33] (Fig. 1). The area under this peak allows the calculation of dipole density, N_d, through the relationship:

$$N_d = \frac{KT_pQ}{\alpha Ap^2Ep} \quad , \tag{1}$$

where Q is the total charge released by the reorientation of the (I-V) dipoles, K is the Boltzmann constant, $\alpha = 1/3$, A is the sample area, p is the dipole moment, and Tp and Ep are the polarization temperature and electric field of polarization, respectively. This measurement is an important one since it gives a precise number of the initial concentration of dipoles. On the other hand, it also allows a calibration of the dipole density vs. the optical absorption coefficient through the following relationship:

$$N_{Eu^{2+}}(ppm) = (12.2\pm0.9)\alpha_{Eu^{2+}}(cm^{-1}) \quad . \tag{2}$$

A comparison between the concentration of isolated (I-V) dipoles as determined from Eq. (1), and the concentration of Eu^{2+} ions obtained from Eq. (2), indicates that after quenching and for concentrations less than ∿350 ppm, all the doubly valent europium ions are in the dipolar state isolated in the matrix.

The X-irradiation in NaCl:Eu^{2+} produces the convertion of Eu^{2+} to the monovalent as well as to the tripositive state. However, the observation of these states is quite difficult and large exposures of X-rays are necessary[36]. Fig. 2 shows the absorption spectrum of a previously quenched europium-doped NaCl crystal (118 ppm) after 9h of room temperature X-irradiation (full curve). Besides the F and M bands, a sharp band peaking at 465 nm superimposed on the F-band, as well as three other very weak absorptions peaking at 880, 965 and 1040 nm can be observed. The former band (465 nm)[38] has been associated with the transition from the ground state ^7F_o of the Eu^{3+} ions tc the excited state $^5D_2$ while the latter have been ascribed to the presence of monovalent europium ions in the irradiated samples[28].

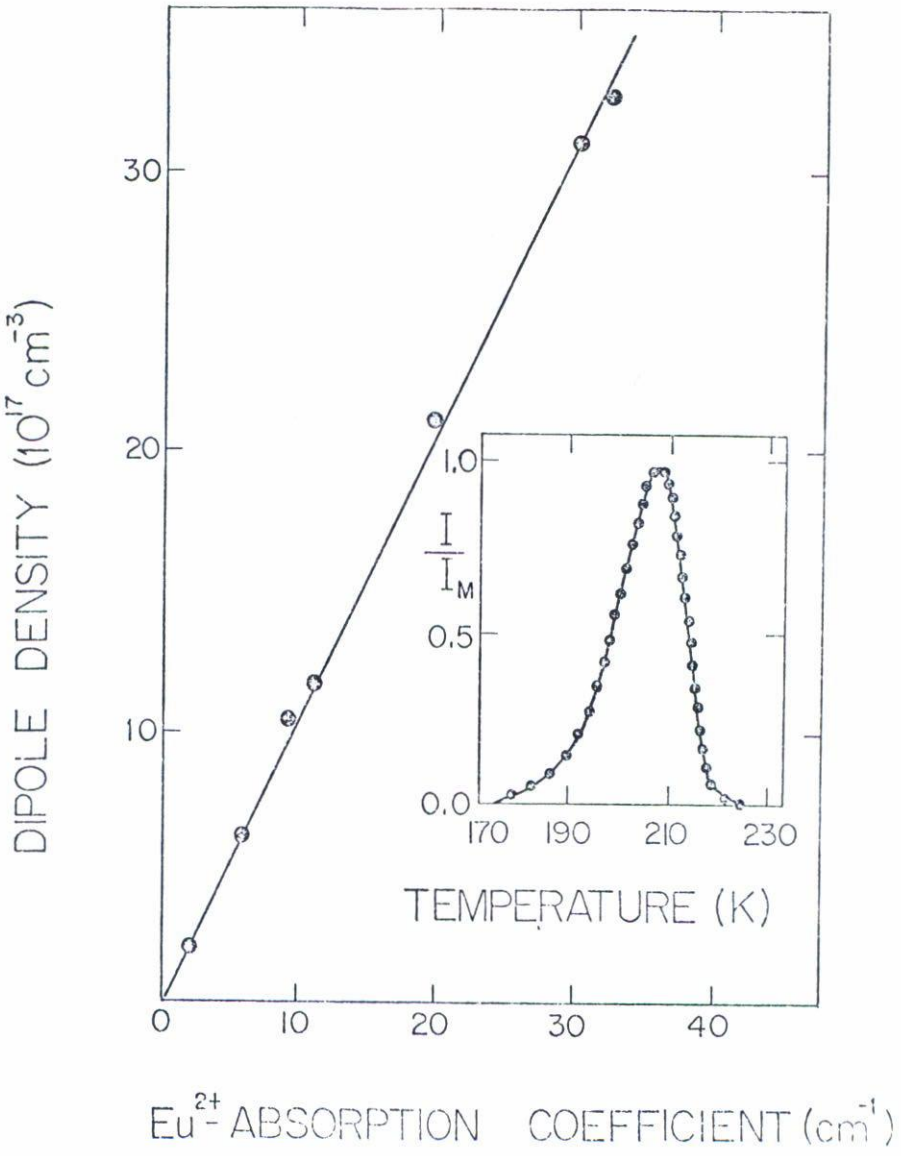

Fig. 1 Dipole density measured by ITC as a function of the absorption coefficient of the 240 nm band in the absorption spectrum of quenched samples of NaCl:Eu^{2+}. The inset show the observed ITC peak (points) as well as the fitting which was performed on this curve using the area method (full curve). (After Rubio et al., Ref. 36).

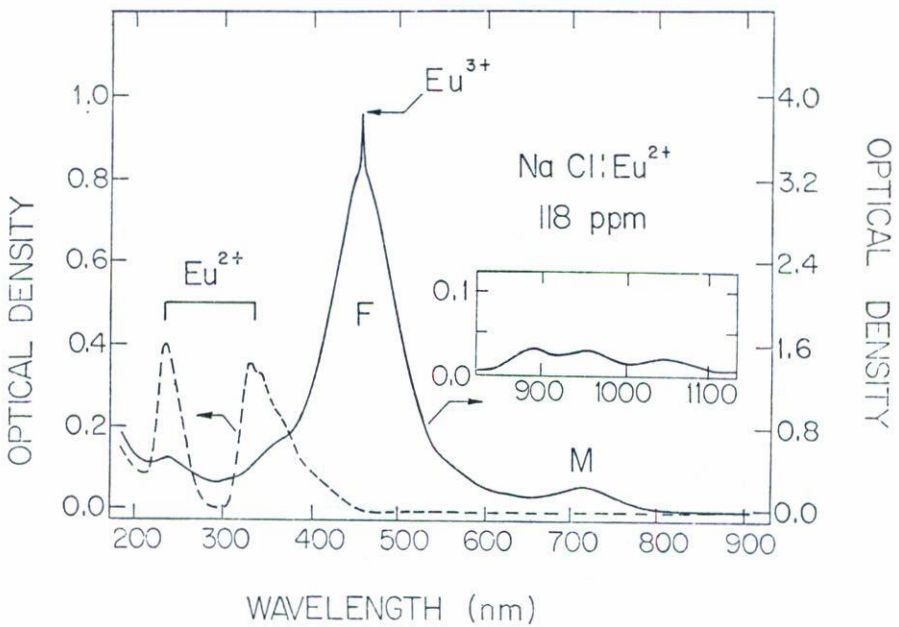

Fig. 2 Optical absorption spectrum of a NaCl crystal doped with 118 ppm of Eu^{2+} after a fast quench from 800 K (broken curve) and after 9h of RT irradiation (full curve). (After Rubio et al., Ref. 36).

Fig. 3 shows the room temperature F-center growth curves as a function of europium concentration for fast quenched samples. From these curves it is possible to obtain the amount of first stage coloration (α_{FO}) by extrapolating the saturation stage of the curves to meet the ordinate. These values plotted against the square root of the total europium concentration are shown in Fig. 4. The curve exhibits a quite good linear dependence for concentrations up to ∿300 ppm. This result is expected from the models given in the introduction. Now, in order to get a deeper insight into the nature of the interstitial halogen traps, the effect of the room temperature X-irradiation on the Eu^{2+} - cation vacancy dipole concentration was analyzed using the EPR technique. It was ascertained that this concentration decreases considerably during the F-center growth. However, the transition from the first to the second stage is

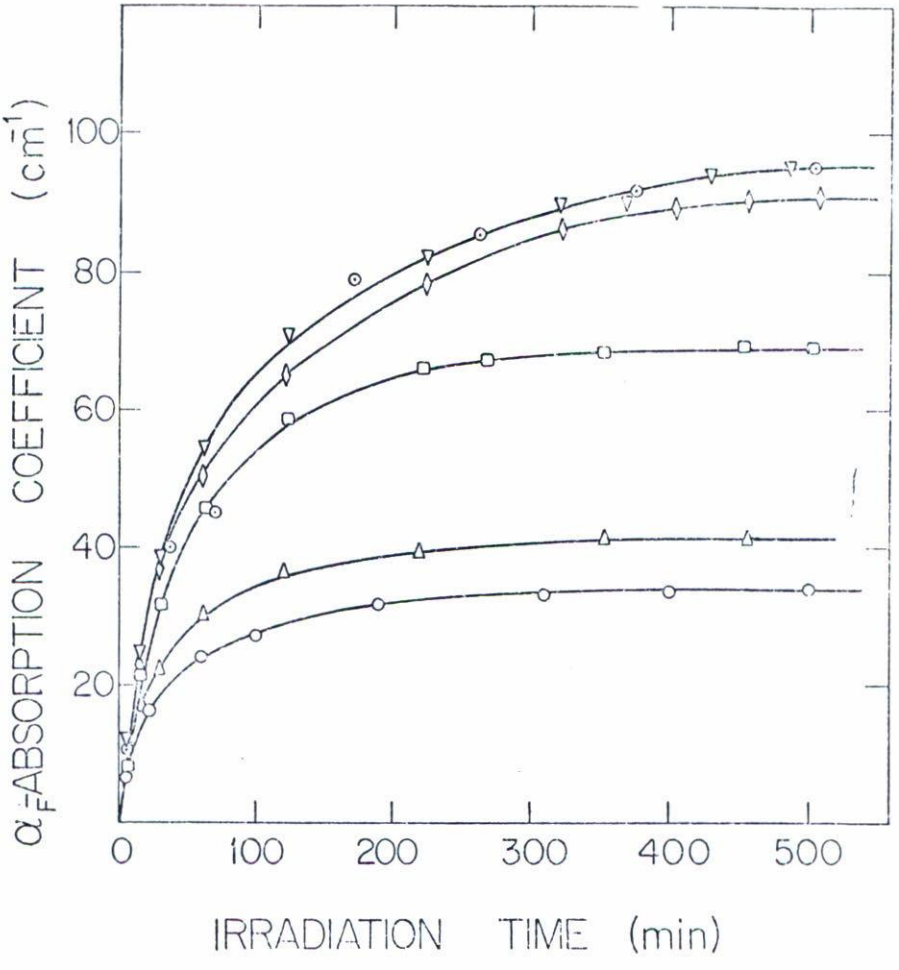

Fig. 3 F-center growth curves as functions of europium concentration for fast quenched samples 0, 29 ppm; Δ, 53 ppm; □, 118 ppm; ◇ , 257 ppm; ▽, 360 ppm; ⊙, 460 ppm. (After Rubio et al., Ref. 36).

not the result of the exhaustion of the dipole concentration. Fig. 5 shows the results obtained for dipole destruction (ΔNd), F-center production (F), and number of doubly valent europium ions which change their valence state by irradiation (ΔEu^{2+}) for two different Eu-concentrations, i.e., 50 and 270 ppm. The values for ΔEu^{2+} were determined from the dif-

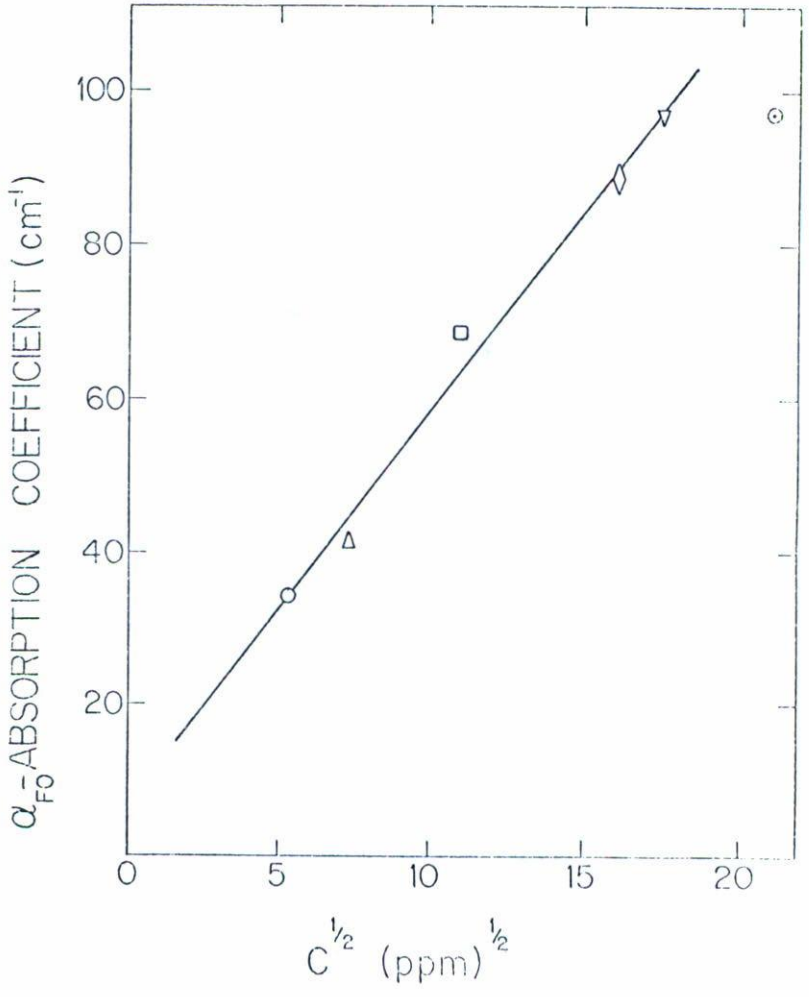

Fig. 4 Relationship between the first stage coloration and the impurity concentration, C. The symbols represent the same Eu concentration as those given in Fig. 3. (After Rubio et al., Ref. 36).

ference between the intensities of the absorption spectrum before and after irradiation. On the other hand, in order to obtain the F-center concentration, a Gaussian band formulation of Smakula's equation was employed, with an oscillator strength of 0.79, while values for ΔNd were obtained following the procedure described above. It is important to point out

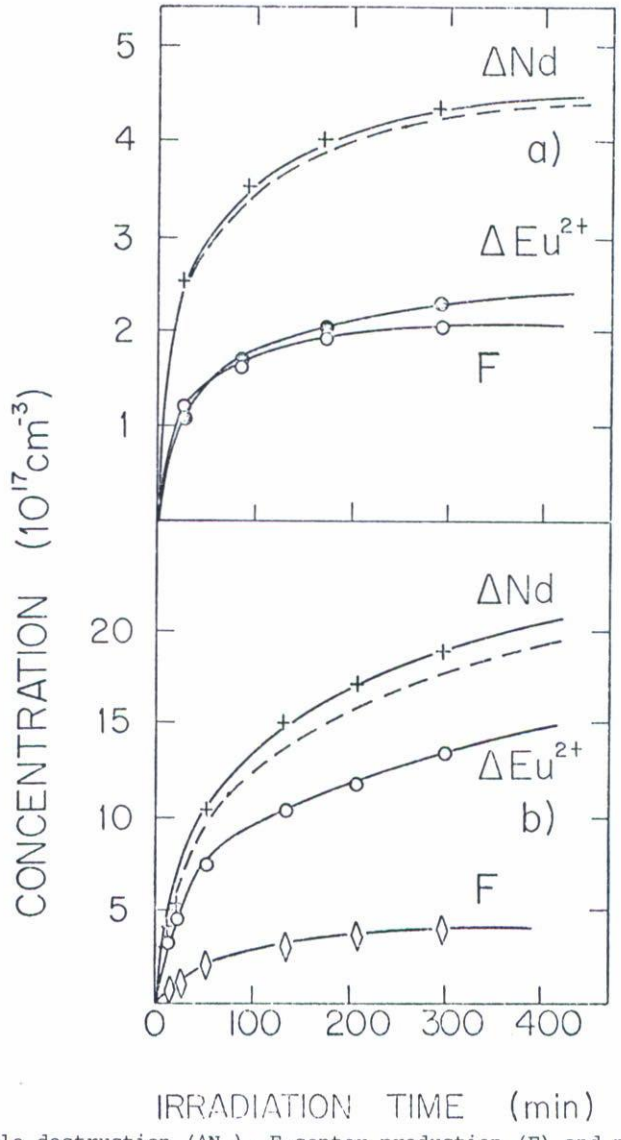

Fig. 5 Dipole destruction (ΔN_d), F-center production (F) and number of doubly valent europium ions which have changed their valence state during irradiation (ΔEu^{2+}).
(a) Sample doped with 50 ppm; (b) 270 ppm. In both cases, the broken curve represents the sum of F and ΔEu^{2+}. The samples were irradiated using X-rays from a tungsten target tube operated at 30 kV and 30 mA filtered through a 1.5 nm aluminium filter. (After Rubio et al., Ref. 36).

that the data for ΔNd were corrected for the dipole aggregation process which occurs at room temperature during the time in which the experiments were performed. Reference to Fig. 5 shows that for the slightly doped sample the number of dipoles destroyed is equal, within experimental error, to the sum of the number of F-centers produced and the number of converted ions. A plot of ΔNd vs. F for the 50 ppm-doped sample shows a linear relationship (Fig. 6) which holds in both the first and second stages of the F-center growth curve which is a result expected if the (I-V) dipoles act as traps for the interstitial defects. At this point, it is important to mention that dipole destruction in europium-doped NaCl can be achieved, however, by two possible mechanisms: a) interstitial trapping and/or b) change of valence state during the irradiation processes. Considering only those dipoles which were destroyed by the former mechanism a linear relationship between ΔNd (corrected) and F was still found as it is shown in Fig. 6 by full symbols. This experimental result points out that the Eu^{2+} - cation vacancy dipoles are the fundamental traps for the radiation induced interstitials given then support to the models for F-center production recently developed by Comins and Carragher[31] and by Aguilar et al.[30].

In contrast with the results given above, it was ascertained that for the more heavily doped sample (270 ppm) $\Delta Nd >> F + \Delta Eu^{2+}$. Moreover, the plot of ΔNd vs. F deviates from the linear behaviour as can be seen in Fig. 6 (shown by full symbols). Similar results have been found by Kao and Perlman[28] in $KCl:Eu^{2+}$ and they suggested that this effect is due to an increase in the dipole aggregation rate produced by the irradiation. To prove if the X-irradiation gives place to this effect EPR and optical absorption intensity measurements were performed in parallel. The results are given in Fig. 7. Reference to this figure shows that the intensity of the EPR signal corresponding to the isolated dipoles decreases faster than the intensity of the optical absorption (OA) signal for both slightly and heavily doped samples. In the former case, the contribution of complexes to the OA but not to the EPR spectra is due to the isolated (I-V) dipoles as well as to those which have trapped an interstitial ion. This latter defect produces only a small perturbation

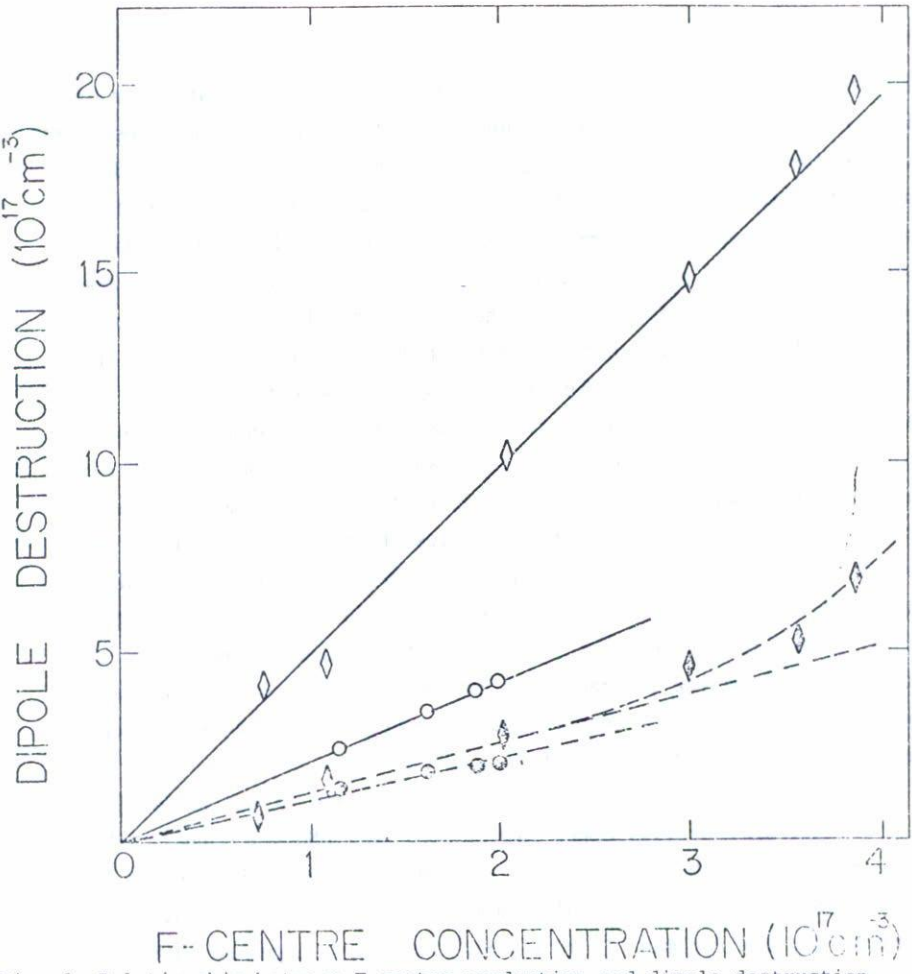

Fig. 6 Relationship between F-center production and dipole destruction as measured by EPR (open symbols): 0, 50 ppm; ◇, 270 ppm. Full symbols represent the same data after subtracting those dipoles which were destroyed because the Eu^{2+} ion forming the complex changed its valence state. (After Rubio et al., Ref. 36).

to the dominant cubic crystal field at the Eu site[35,37], not altering them, significantly, the absorption and emission spectra of the (I-V) dipoles, i.e., the optical bands associated with (I-V) dipoles and dipoles with an interstitial ion trapped must be superimposed. On the other hand, since the interstitial halogen ion is a paramagnetic defect, it is expec-

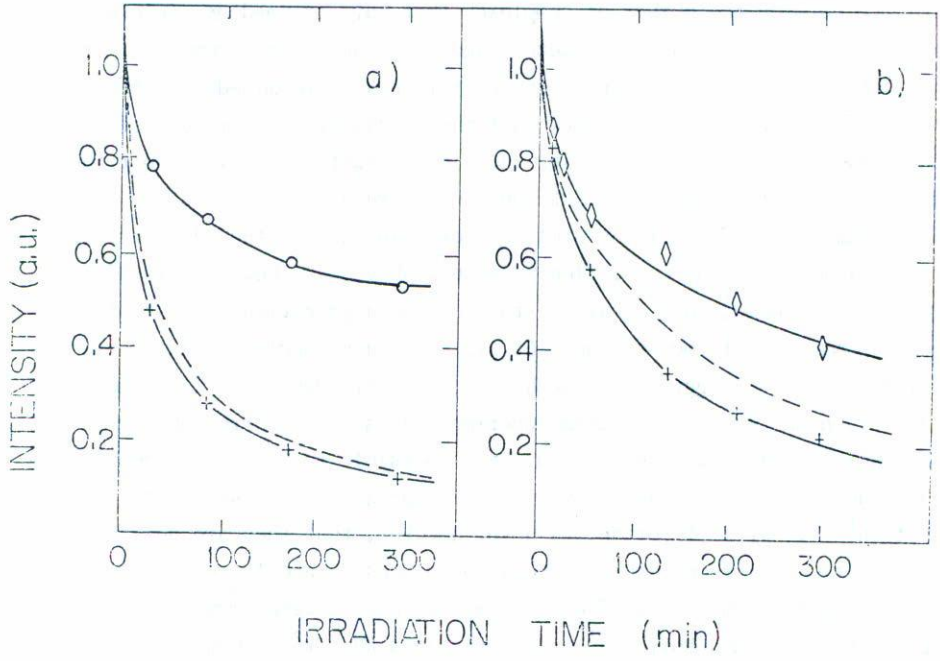

Fig. 7 Decay in intensities of the EPR(+) and optical absorption spectra (0, ◊) as function of the irradiation time: (a) 50 ppm; (b) 270 ppm. The broken curve represents the decay in intensity of the absorption spectrum after subtracting the number of dipoles which have trapped the interstitial defects. (After Rubio et al., Ref. 36).

ted that the complex formed by this ion and the dipole have a rapid spin-lattice relaxation and the EPR spectrum of this complex may not be detected at room or even at liquid nitrogen temperatures. The data presented in Fig. 6 indicate that one halogen interstitial ion is trapped at the (I-V) dipoles. This is also supported by the calculations performed by Aguilar et al.[16], who show that the average number of defects trapped at the isolated dipoles is close to one for the impurity concentration range used in this work. Under this assumption, the number of dipoles that have trapped one interstitial ion equal to the number of F-centers produced. Now, since the concentration of Eu^{2+} - vacancy complexes is equal to the total concentration of Eu^{2+} ions before irradiation, the dif-

ference between the number of complexes that have trapped one interstitial and the Eu^{2+} concentration as determined from the OA spectrum after irradiation, should give the dipole concentration as determined from the EPR spectra. Rubio et al.[36] found that these assumptions were correct as shown by the dashed curve in Fig. 7a. In contrast with this result the decrease in intensity of the EPR spectrum corresponding to the heavily doped sample was found to be still faster than that of the OA spectrum, even after making the correction mentioned above, as shown in Fig. 7b. On the other hand, in a detailed study on the aggregation process of Eu^{2+} ions in NaCl, performed by López et al.[37], they concluded that the first products of aggregation such as dimers, trimers, etc. have their absorption and emission spectra superimposed on those corresponding to the isolated (I-V) dipoles. Then, it is possible to conclude from the data shown in Fig. 7b that this type of complexes are present after irradiation[36]. It is important to note, however, that they are not the result of the room temperature aggregation process since ΔN_d was corrected to take into account this effect. Similar results were previously reported by Muccillo and Rolfe[29] in γ-irradiated $KBr:Sr^{2+}$. However, Rubio et al.[36,39] were the first to gather experimental evidence to show that an increase in the dipole aggregation rate is really produced by the X-irradiation.

The room temperature X-irradiation $NaCl:Eu^{2+}$ work has been discussed in more or less detail because the Eu^{2+} ion allows the simultaneous use of several techniques which give a more complete view of the induced radiation damage.

Similar results as those discussed above have been found for lead-doped sodium chloride by García et al.[40] In this system dipole destruction was monitored by the ITC technique while the number of ions that change valence were determined through the optical absorption band peaking at 273 nm. Fig. 8 shows the results obtained for dipole destruction, F-center production and number of converted ions for 120 and 220 ppm lead- concentrations. The analysis of these results allowed the conclusion that the Pb^{2+} - cation vacancy dipoles are the dominant traps for the radiation induced interstitials. For the 220 ppm doped sample the re-

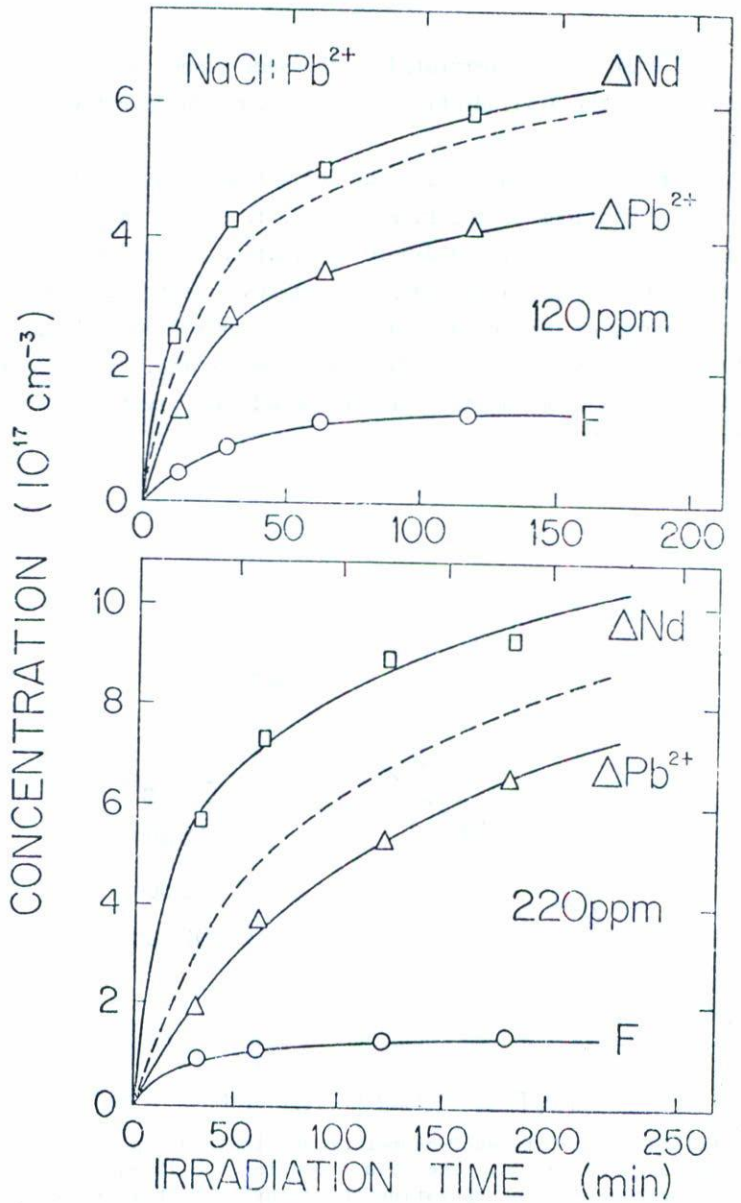

Fig. 8 Dipole destruction (ΔN_d), F-center production (F) and number of Pb^{2+} ions that have changed valence state by irradiation (ΔPb^{2+}). (a) Sample doped with 120 ppm; (b) 220 ppm. In both cases the broken curve represents the sum of F and ΔPb^{2+}. All data were taken operating the X-ray tube at 30 kV and 20 mA. (After García et al., Ref. 40).

sult $\Delta N_d >> F + \Delta Pb^{2+}$ was interpreted in the same manner as above, i.e., considering that the X-irradiation increases considerably the dipole aggregation rate.

García et al. have also analyzed the NaCl:Ca^{2+} system, founding that for concentrations in the range from 15 to 90 ppm there exists a proportional relationship between dipole destruction and F-center production which holds in both the first and second stages of the F-center growth curve; the number of dipoles destroyed per F-center created being close to unity as can be seen from the data presented in Fig. 9. This result is similar to that found in the europium-doped NaCl crystal[36].

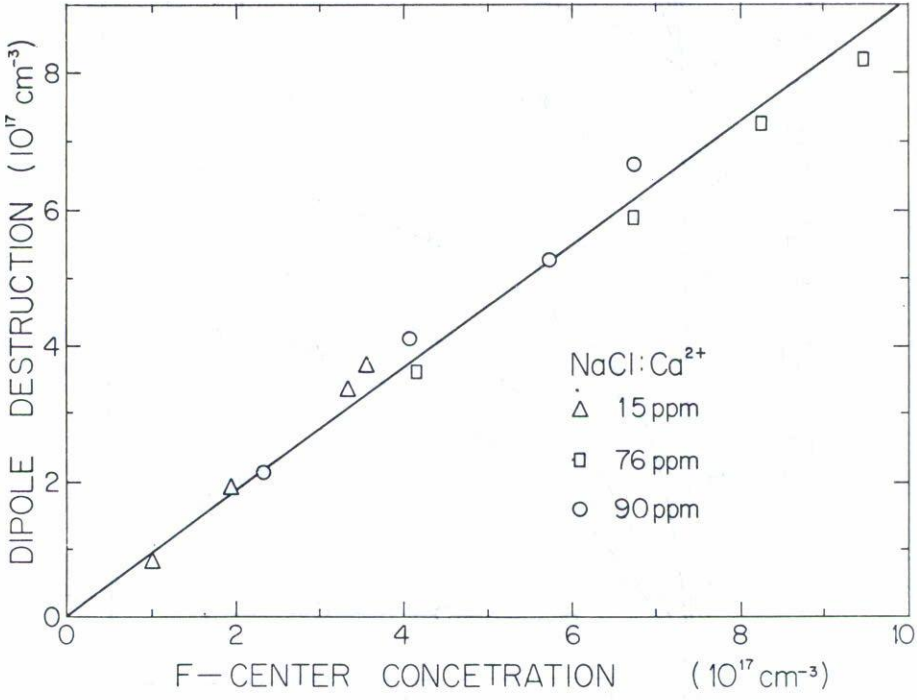

Fig. 9 Relationship between F-center production and dipole destruction as measured by ITC. The data shown for the 15 and 90 ppm doped samples were taken operating the X-ray tube at 20 kV and 20 mA, while that for the 76 ppm were taken at 30 kV and 20 mA. (After García et al., Ref. 40).

At this point, we may conclude that the results discussed above

for both europium, lead, and calcium-doped sodium chloride give strong support to the models developed by Comins and Carragher and Aguilar et al. and give evidence that the (I-V) dipoles are the dominant traps for the mobile interstitial defects.

On the other hand, these theoretical models predict not only that the efficiency for coloring must be proportional to the square root of impurity concentration but also to the square root of dose rate (g). This prediction has been recently confirmed by Ramos et al.[41] in several systems and the results are displayed in Fig. 10. It should be noted that the models for F-center growth were developed for ions which do not change their valence state by irradiation. However, the linear dependence between F_s and $\sqrt{g}$ was also experimentally found to hold even for an ion like Eu^{2+} which is well known that change its valence state during irradiation.

b) Influence of the second phase precipitates on the F-coloring efficiency

It can be appreciated from the data shown in Fig. 4 that for Eu-concentrations higher than ∿350 ppm, the amount of first stage coloration is smaller than the expected from the linear dependence predicted by the theory. Similar results have been reported for KCl:Sr^{2+}[42], KCl:Pb^{2+}[43] and NaCl:Mn^{2+}[15] by other workers. In these systems it has been observed that the higher the concentration, smaller is the saturation level in the F-center growth curve. This fact may be explained if one takes into account that for high concentrations the quenching treatment does not prevent impurity precipitation. In fact, for the particular case of NaCl-Eu[36], it has been ascertained that for high concentrations (∿350 ppm), the quenched samples usually present second phase precipitates. These structures may not be as efficient as the (I-V) dipoles for the trapping of the halogen interstitial defects and therefore their presence may introduce significant changes in the F-coloring efficiencies of the crystal.

In order to study the influence of the second phase precipitates of divalent cation impurities on the F-coloring efficiency, Medrano and coworkers[44] have recently analyzed the systems NaCl:Pb^{2+} and NaCl:Sr^{2+}.

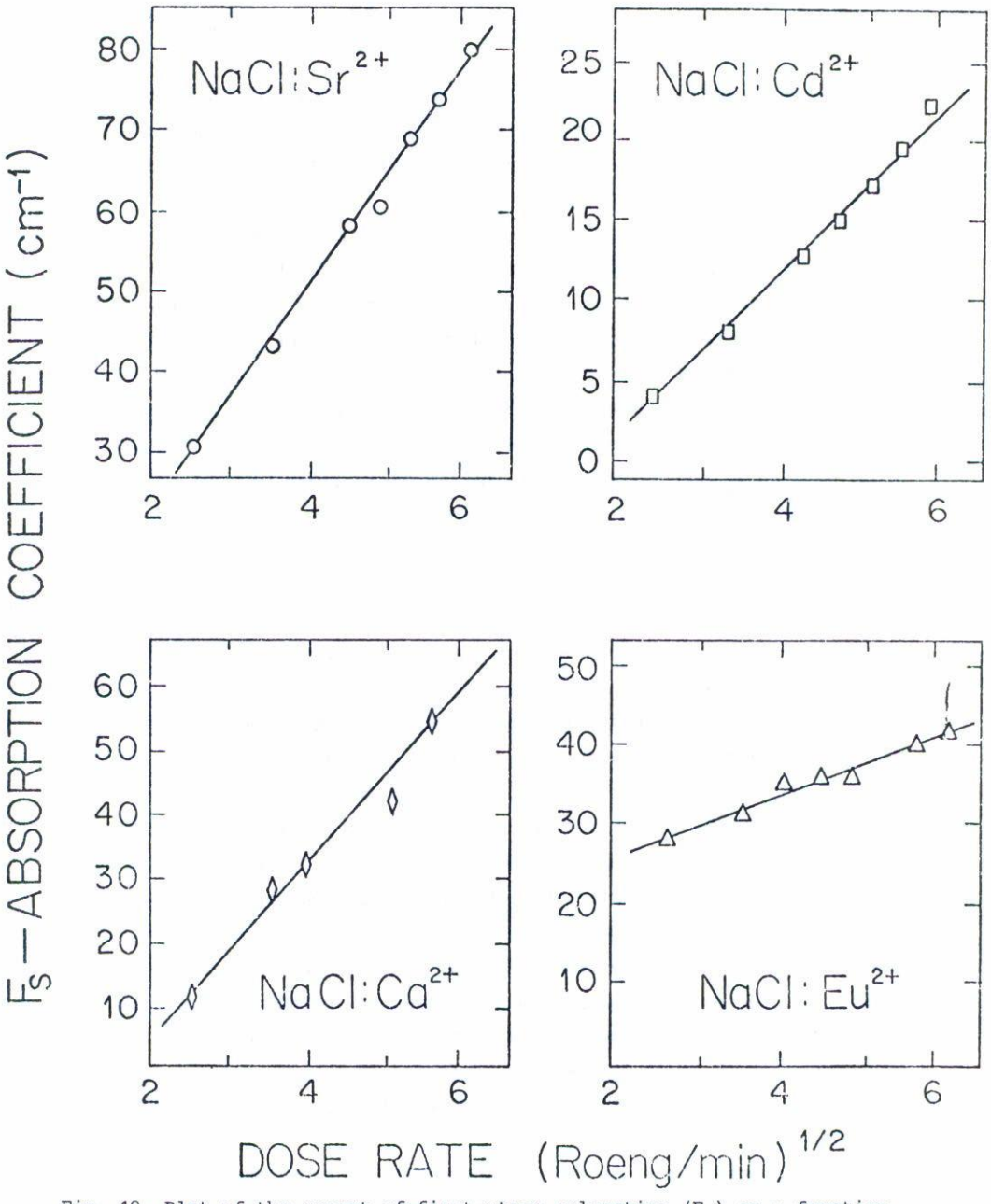

Fig. 10 Plot of the amount of first stage coloration (F_s) as a function of the square root of X-irradiation dose rate. (After Ramos et al., Ref. 41).

It is well known that the optical absorption bands of Pb^{2+} are quite sensitive to the aggregation-precipitation state of this ion in the NaCl matrix[45-47]. In particular, after a fast quench from high temperatures, there is a prominent band peaking at 273 nm in the absorption spectrum which has been ascribed to Pb^{2+} - cation vacancy complexes isolated in the lattice. Aging at room temperature, however, produces the appearance of two other bands peaking at 264 and 287 nm whose intensities grow at the expense of that observed immediately after quenching. The 264 nm band has been associated with the presence of the stable dihalide phase $PbCl_2$ in the aged crystals while the one peaking at 287 nm has been recently ascribed to a metastable lead precipitate in the {110} plane[47]. The evolution of the intensities of those bands as a function of the annealing time at room temperature is shown in Fig. 11. On the other hand, in order to study the influence of these second phase precipitates on the F-coloring efficiency of NaCl, the samples were first quenched from 550°C to room temperature and then annealed at 23°C for different periods of time and irradiated under the same conditions. The irradiation time was selected to bring the coloring to an intermediate point on stage I of the F-center production. Therefore, the F-absorption coefficient can be taken as a measure of the average efficiency for stage I. Reference to Fig. 11 shows that the first hours of annealing produce an increase in the F-coloring efficiency up to ∿25h, time during which, the metastable phase responsible for the absorption band peaking at 287 nm grows. At longer times the stable dihalide phase nucleates, producing a smaller increase in the F-coloring than the one produced during the first hours of annealing.

On the other hand, the annealing at 300°C produces the stable precipitate $PbCl_2$ with a characteristic absorption band at 264 nm. Measurements similar to those above, revealed that the F-coloring efficiency decreases only slightly with respect to the value measured immediately after quenching up to ∿20h, this decrease being correlated with the growth of $PbCl_2$ precipitates in the NaCl matrix. For longer annealing times, there is a saturation in the F-coloring efficiency as well as of the intensity of the 264 nm band. Samples with different thermal treat-

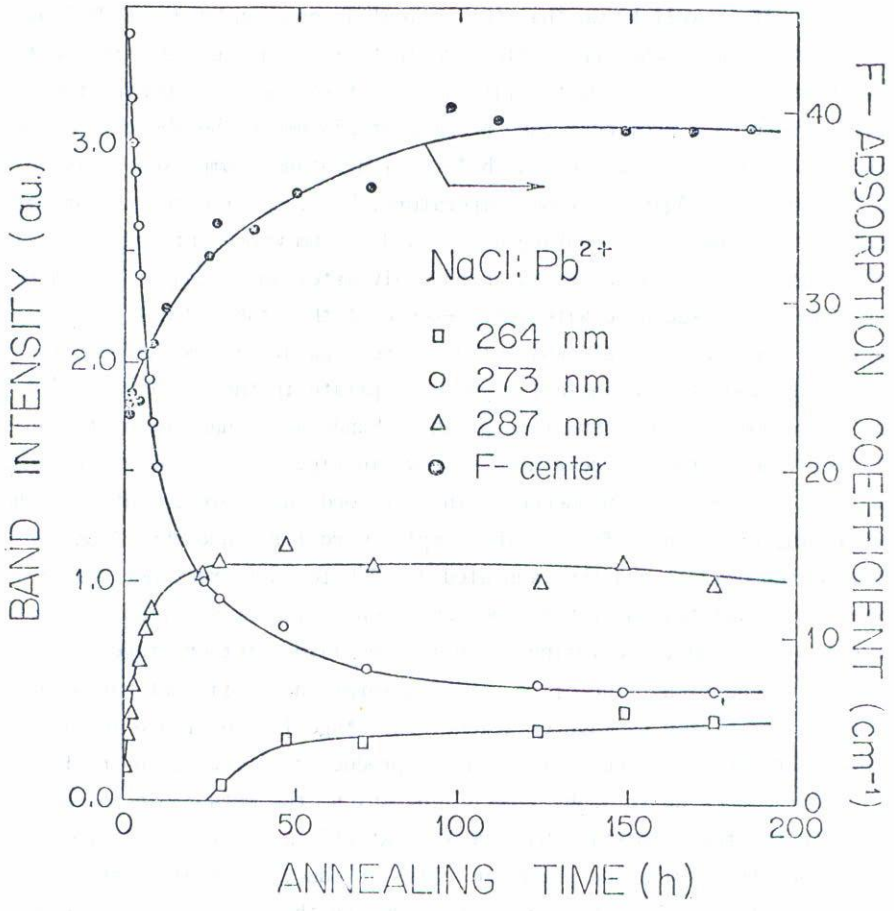

Fig. 11 Efficiency of coloring in Pb^{2+} doped NaCl as a function of the annealing time at RT. The evolution of the intensities (area under the curve) of the different absorption bands which develop during the aging at this temperature is also included. (After Medrano et al., Ref. 44).

ments but irradiated under the same conditions (200 min) showed that the F-absorption coefficient (α_F) for a sample aged at 23°C for 200h was about 4 times greater than the one for a "pure" sample. For a freshly quenched crystal however this factor was about two, while for a sample annealed at 300°C for 300h the value for (α_F) is just 1.7 greater than the

one for the "pure" one. These results give evidence that the different precipitated phases contribute in a quite different manner to the coloring efficiency. The complete coloring curve for these samples show that for any irradiation time the efficiency for coloring of the metastable lead precipitate is higher than that of the isolated dipoles or than that of the stable $PbCl_2$ phase (Fig. 12).

Another system which was investigated is NaCl:Sr^{2+}. In this particular case, as the impurity ion does not present optical absorption bands, an optical probe was used to monitor the strontium precipitation processes occurring in the NaCl host. This probe was the Eu^{2+} ion which as it has been discussed before, presents several advantages over other ions. The use of Eu^{2+} as an optical or magnetic probe has been previously investigated[48,49]. The aging at 280°C produces two Sr-metastable precipitates associated with two emission bands peaking at 415 and 450 nm from which grows the stable dihalide phase $SrCl_2$ associated with the emission band peaking at 407 nm. The evolution of these bands as a function of the annealing time at 208°C is presented in Fig. 13. The band peaking at 429 nm is the promient one immediately after quenching, growing the other bands as a function of the annealing time at the expense of this one. Fig. 13 also includes the F-coloring efficiency, which increases very rapidly during the first hour of annealing as the intensities of the emission bands associated with the metastable phases increase. Al longer annealing times the intensities of these latter bands decrease simultaneously with the F-coloring efficiency. After 200h of annealing the only precipitate present in the sample is the $SrCl_2$ phase which reduces the coloring efficiency by about 40% relative to the value measured after quenching. The observed initial increase in the F-absorption coefficient relative to the value after quenching points out the higher efficiency of the metastable phases for the trapping of the radiation induced interstitials than the stable precipitated phase[44].

The annealing of quenched samples at room temperature produces different precipitates from those at 280°C. In fact it is observed the growth of an emission band peaking at 416 nm due to Eu^{2+} ions embedded into a metastable Sr-precipitate from which grow those associated with

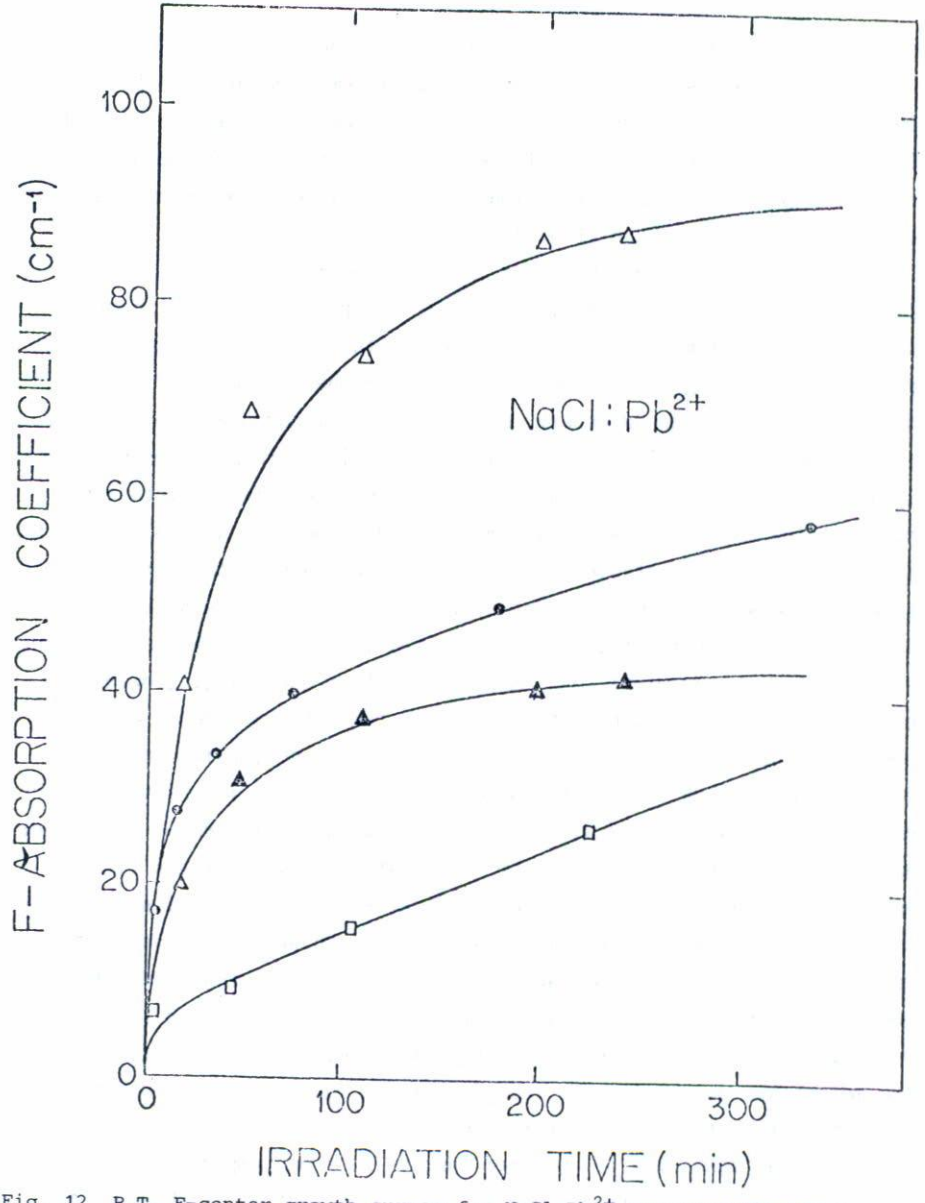

Fig. 12 R.T. F-center growth curves for NaCl:Pb^{2+} corresponding to a freshly quenched crystal (●), a sample annealed at 23°C for 200h (Δ), a crystal aged at 300°C for 300h (▲), and the one obtained from a nominally pure sample (□). (After Medrano et al., Ref. 44).

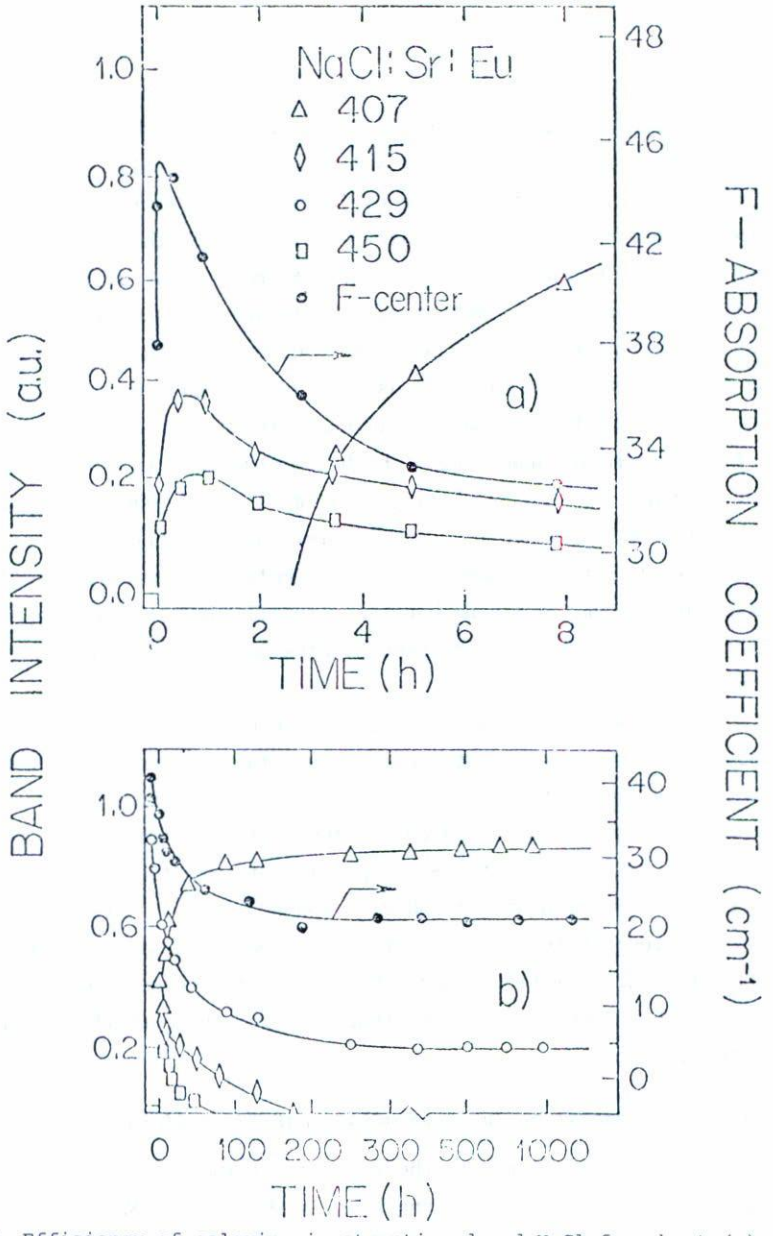

Fig. 13 Efficiency of coloring in strontium doped NaCl for short (a) and long (b) annealing times at 280°C. The evolution of the intensities of the Eu-emission bands which develop during this annealing treatment is also included for comparison. (After Medrano et al., Ref. 44).

the emission bands peaking at 410 and 448 nm. On the other hand, EPR studies[48] indicated that the precipitate associated with the band at 410 nm posseses a cubic structure, its lattice being parallel to the {100} plane of the NaCl matrix. The excitation spectra of these two latter bands allowed the conclusion that the structure of the strontium second phase precipitate associated with the 448 nm band was different to that of $SrCl_2$, as well as from that of the precipitate associated with the emission band peaking at 410 nm. The evolution of the intensities of these bands is shown in Fig. 14, as well as the measured F-coloring efficiency. The results for this efficiency are clearly different from those obtained from the annealing at high temperature. In particular, the value obtained for the F-coloring ($\sim$71 cm^{-1}) after 1000h is $\sim$69% higher than the one obtained ($\sim$22 cm^{-1}) after the same time of annealing at 280°C. Nevertheless, it appears that the metastable precipitated phase associated with the 416 nm band is more efficient in the trapping of the interstitial ions than the precipitates associated with the 410 and 448 nm bands[44].

Fig. 15 shows in a more clear way the effect described above. The F-coloration curves were obtained from crystals: a) annealed 1700h at RT, in which the precipitates associated with the bands peaking at 410 and 448 nm were the only ones present at the start of irradiation; b) annealed 1000h at 280°C, where the $SrCl_2$ precipitate was the only one present at the start of irradiation; and c) a "pure" sample. These curves show that the precipitates produced at room temperature are more efficient traps for the radiation induced halogen atoms, reassuring the proposition that they have a different structure from those which nucleate at high temperatures.

c) *Effects of X-irradiation in other alkali halide crystals*

For the sake of brevity the results obtained for other alkali halides will not be discussed at length as in the case of NaCl, since they are quite similar and only some of the more important points will be mentioned.

Europium-doped KCl[39] showed the usual behavior with regard to

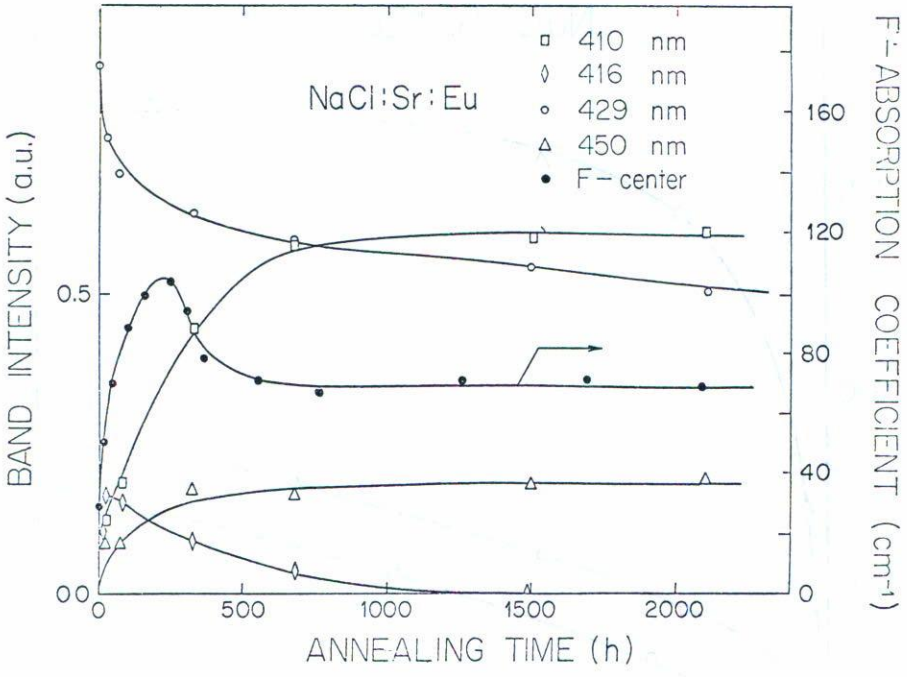

Fig. 14 Efficiency of coloring as a function of Sr-precipitation in NaCl at 23°C. The evolution of the intensities of the Eu-emission bands which develop during this annealing treatment is also included. (After Medrano et al., Ref. 44).

the F-coloring curves, consisting of the two well known stages of coloration, an early fast first stage and a late slow second stage. Also, the coloring increased in a monotonic way as the Eu-concentration increases up to ∿600 ppm. The relationship between the amount of first stage coloration and the square root of impurity concentration is linear for concentrations up to ∿600 ppm.

On the other hand, the nature of the interstitial traps in this system has been also analyzed in considerable detail. Fig. 16 shows the results obtained for dipole destruction, F-center production, and number of Eu^{2+} ions which have changed their valence state by irradiation for two Eu-concentrations, 180 and 580 ppm. As in the system NaCl:Eu^{2+}, the results are in agreement with the expectation $\Delta Nd >> F + \Delta Eu^{2+}$, according

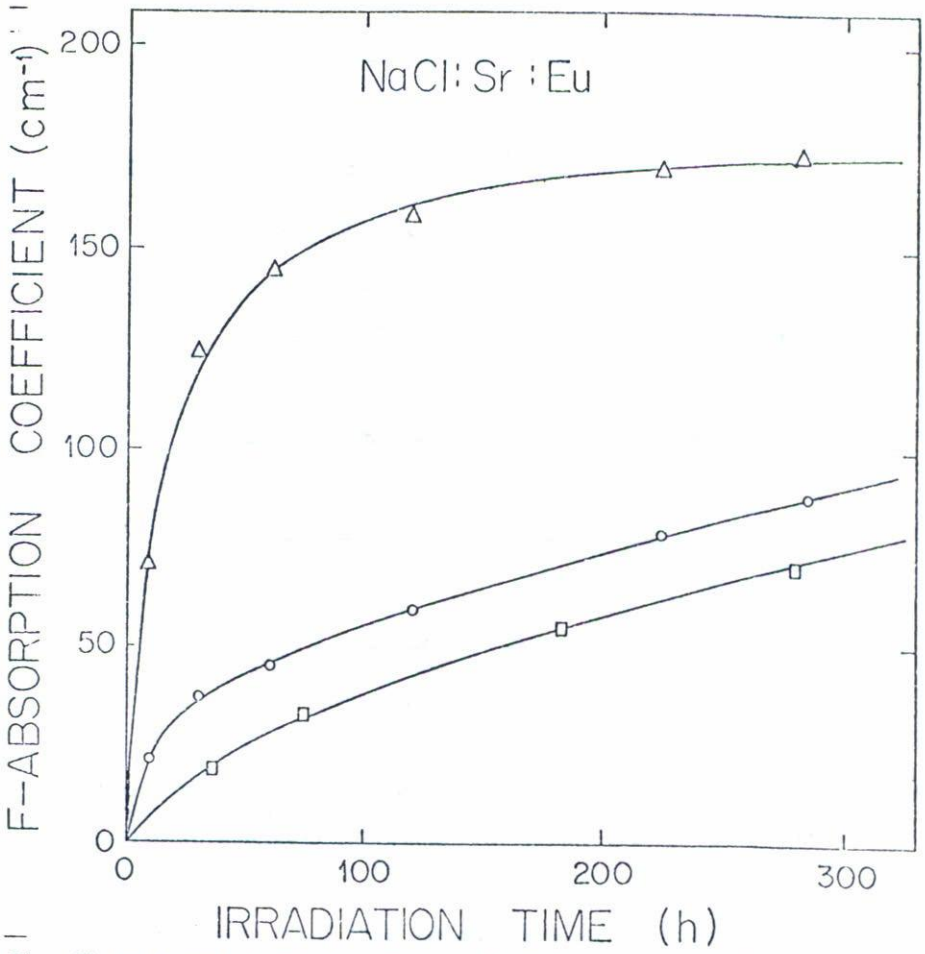

Fig. 15 RT F-center growth curves for NaCl:Sr:Eu corresponding to a crystal which was aged at 23°C for 1700h (Δ), a sample annealed at 280°C for 1000h (o), and the one obtained from a nominally pure sample (□). (After Medrano et al., Ref. 44).

to Comins and Carragher and Aguilar et al.'s models.

It is important to mention that although in the present paper results obtained in the system KCl:Eu^{2+} have been discussed after those in NaCl:Eu^{2+}, the work on KCl:Eu^{2+} was the first one to gather enough experimental evidence to show that the dipole aggregation rate is increased by irradiation. This was possible thanks to the simultaneous use of the

optical absorption, photoluminescence, ionic thermocurrents and electron paramagnetic resonance techniques.

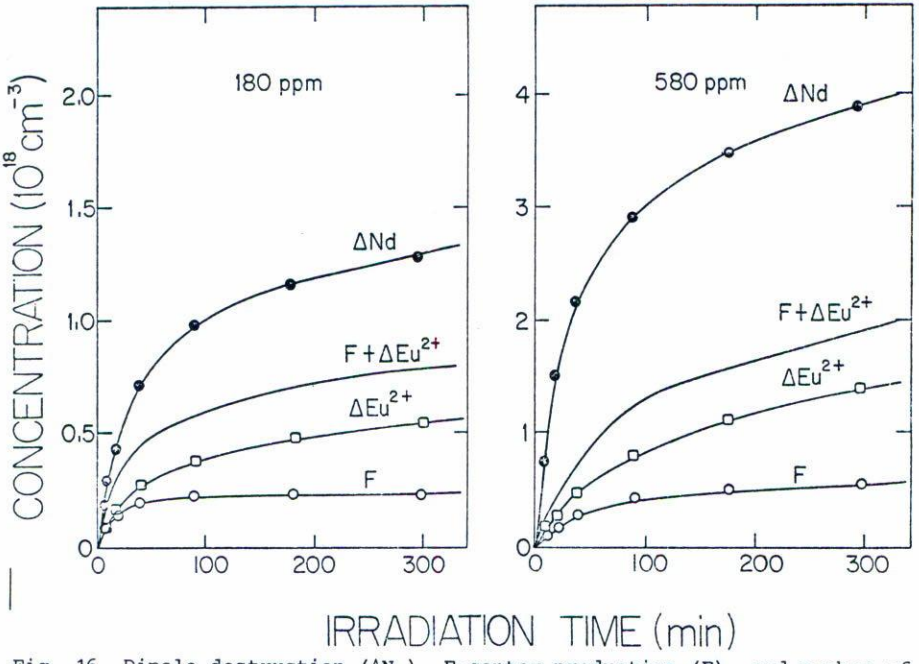

Fig. 16 Dipole destruction (ΔN_d), F-center production (F), and number of divalent europium ions which have changed their valence state (ΔEu^{2+}) during irradiation. (After Rubio et al., Ref. 39).

Figs. 17 and 18 show the F-coloring efficiency as a function of the formation of the different europium second phase precipitates in the KCl matrix. In particular, the annealing of quenched samples at temperatures in the range 23-100°C produces the nucleation of the Suzuki phase responsible for an emission band peaking at 427 nm[37]. The annealing at 200°C, however, produces two metastable precipitates from which grows the stable dihalide phase $EuCl_2$[50]. The Eu^{2+} ions included in the former two precipitates give emission bands peaking at 439 and 478 nm, respectively while in the latter case a band at 410 nm is observed. The evolution of the intensities of those bands as a function of the annealing time at 100 and 200°C is also displayed in the figures for the sake of comparison. The results for the annealing at the former temperature in-

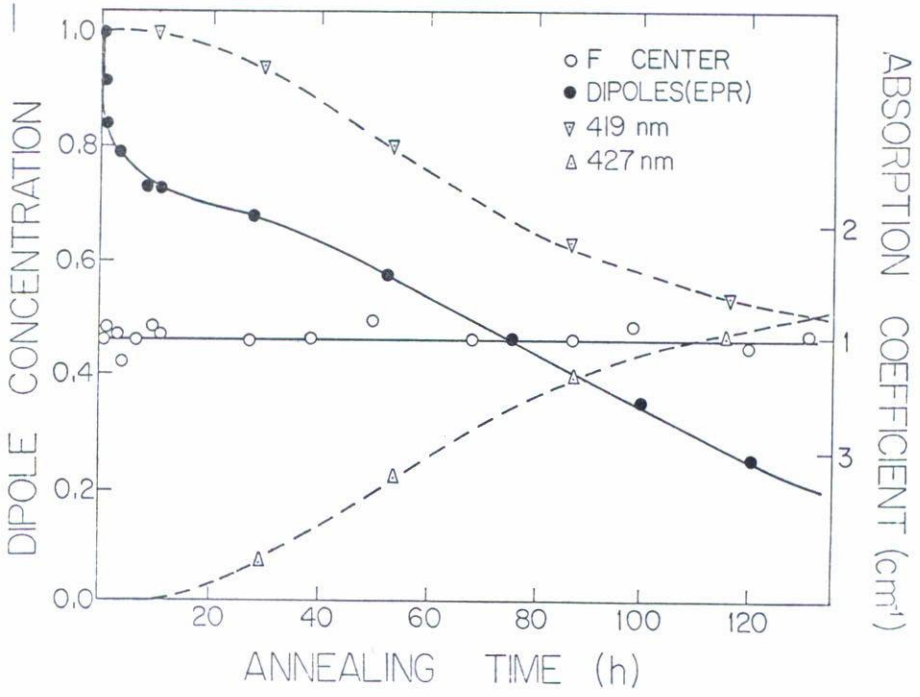

Fig. 17 Efficiency of coloring (normalized to unit) as a function of the aging time at 100°C. Dipole decay, as well as the intensities of the emission bands peaking at 419 and 427 nm are also included for comparison. (After Rubio et al., Ref. 39).

dicate that the initial rate of coloring is independent of the precipitation of the impurity up to ∿120h, even when a considerable amount of Eu^{2+} ions has been precipitated to form the metastable phase. However, the coloring curve for a sample in which almost all the impurity is precipitated into the Suzuki phase, as revealed by the emission spectrum, shows a slightly higher coloring rate than that corresponding to a sample in which the isolated impurity vacancy dipoles are the only ones present. At variance with this result, the aging at 200°C produces a considerable influence in the initial efficiency for coloring and it decreases as a function of the annealing time. After 1200h the efficiency is quite similar to that measured in a nominally "pure" sample. These results may suggest that the Suzuki phase is contributing to the coloring in a quite similar

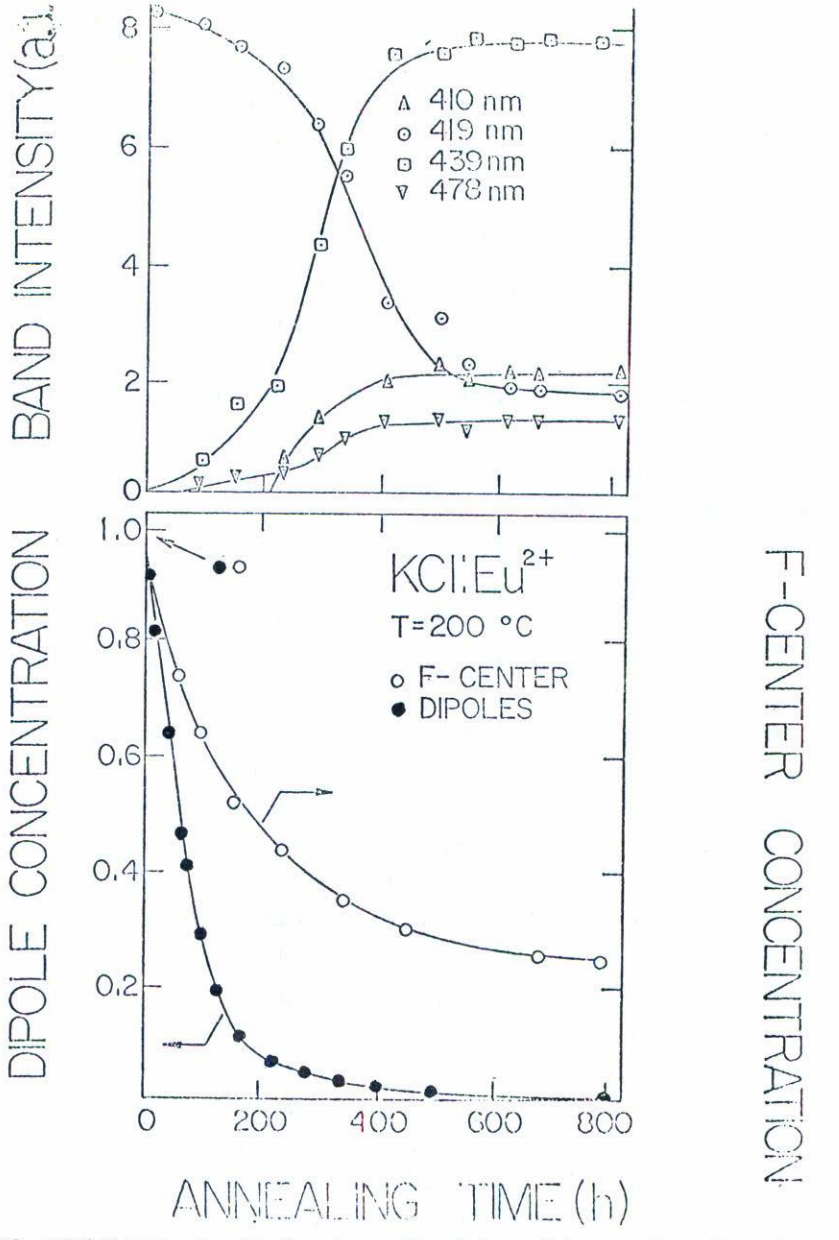

Fig. 18 Efficiency of coloring (normalized to unit) as a function of the aging time at 200°C. Dipole decay as well as the evolution of the intensities of the emission bands peaking at 410, 478 nm are included for the sake of comparison. (After Rubio et al., Ref. 39).

manner as the isolated (I-V) dipoles, while precipitates with the $EuCl_2$ structure have a lower capability to trap the radiation induced interstitials[39].

d) Effect of X-irradiation on the precipitated phases

To understand the effects produced by irradiation on materials which could be used in nuclear reactors, a lot of effort has been put to investigate solute redistribution in alloys during irradiation. It has been shown that irradiation can both order or disorder two phase systems depending on the irradiation conditions and on the nature of the alloy. Ordering effects have been generally found to be produced by electrons and thermal neutrons, while disordering usually is produced by fast neutrons and heavily charged particles.

On the other hand, as far as we know, the stability under irradiation of metastable and stable precipitates of divalent cation impurities in alkali halides, however, has not been investigates up to date. The equilibrium conditions, set solely by thermodynamics, in an irradiation environment must be perturbed, since this can influence both the precipitate dissolution rate and the solute diffusion coefficient. These changes in the equilibrium conditions, due to changes in the precipitation stability have been investigated by Aguilar et al.[51,52].

When a well-aged crystal is exposed to X-irradiation, the emission spectrum of europium-doped NaCl suffers some changes. The emission spectra of a NaCl crystal, aged for 8 years at RT, doped with 600 ppm of Eu^{2+} before irradiation consists of four Gaussian-shape bands; one peaking at 427 nm ascribed to (I-V) dipoles as well as to the first products of aggregation, one at 410 nm associated with the stable precipitate $EuCl_2$, and two others peaking at 439 and 485 nm related to metastable $EuCl_2$-like plate zones[37]. The effect of the X-irradiation can be clearly appreciated in Fig. 19. The irradiation tends to destroy the pre-existing metastable $EuCl_2$-like plate zones producing an enhancement of the 427 nm band, as well as an increase in the europium precipitation into the $EuCl_2$ phase. The enhancement of the 427 nm band is due to small aggregates generated by the dissolution of the metastable precipitates

during irradiation. This conclusion was achieved through EPR measurements, which showed an intensity decrease of the signal ascribed to the few isolated (I-V) dipoles still in solution rather than an increase in this signal. In fact the EPR spectrum associated with the few (I-V) dipoles disappeared after ∿2h of irradiation.

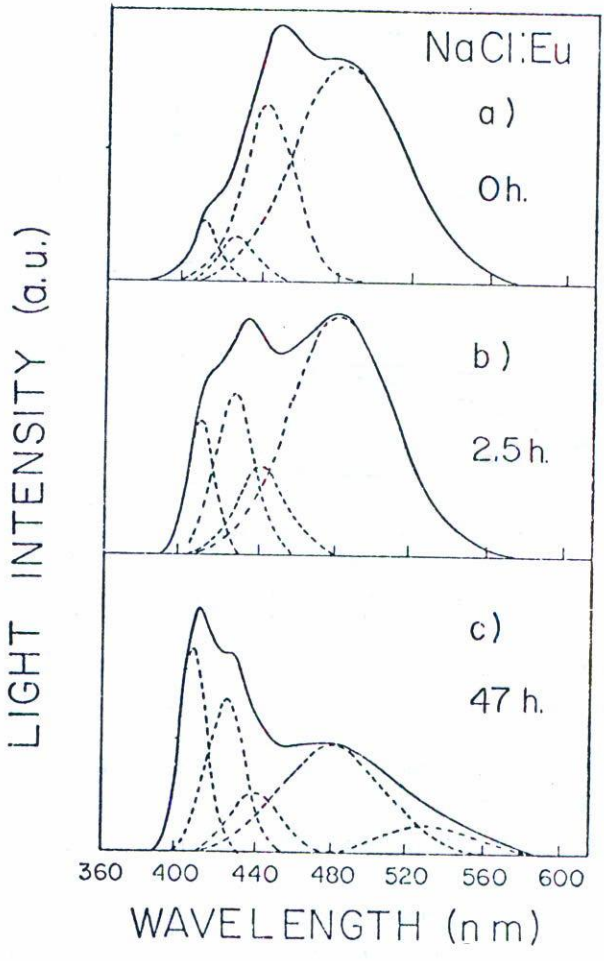

Fig. 19 Fluorescence spectrum of a well-aged sample of NaCl:Eu^{2+} (600 ppm) as a function of the room temperature X-irradiation time. (After Aguilar et al., Ref. 51).

The band peaking at 427 nm increased up to ∿20h of irradiation time and then decreased while the one peaking at 410 nm grows monotonically. The results are shown in Fig. 20. This may suggest that there is a net flow of solute resulting from the ripenning of the metastable phase, to the $EuCl_2$ phase through a diffusion mechanism enhanced by the X-irradiation.

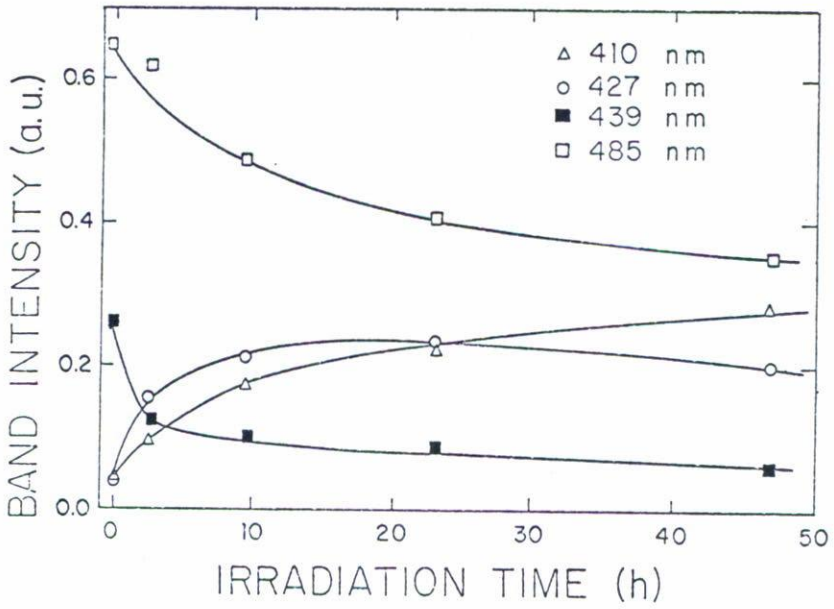

Fig. 20 Evolution of the intensity (area under the curve) of the emission bands of Eu^{2+} in NaCl. (After Aguilar et al., Ref. 51).

At this point it should be mentioned that high doses of X-irradiation also produced the growth of an emission band peaking at 535 nm which had not previously been observed during the annealing treatments in the range of temperatures (25-200°C). The excitation spectrum of this band showed that Eu^{2+} ions are involved in this emission. The origin of this band is still uncertain at the moment, but it might be correlated with clusters of Eu^{2+} and interstitial halogen defects or with the presence of a second phase precipitate whose structure may be different to those of the precipitates generated by annealing in the temperature range

(25-200°C).

The influence of the X-irradiation on the Eu-precipitated phases in other alkali halides is presented in Table I. The main effect is that the radiation tends to destroy the metastable phases enhancing the EuX_2 (X = halogen ion) second phase precipitate producing first small aggregates such as dimers, trimers, etc. which through a diffusion mechanism are incorporated into the stable dihalide phase.

The effect of the precipitated phases of Eu^{2+} in the alkali halides on the coloring efficiency are given in Table II.

TABLE I

Host	Peak position of the emission band in nm	thermal treatment	Assignation	Effects of X-irradiation	Ref.
KI	450	270°C	Metastable phase	destroyed	
	470	270°C	Metastable phase	destroyed	53
	421	270°C	EuI_2-phase	enhanced	
NaBr	453	RT	Metastable phase	destroyed	
	487	RT	Metastable phase	destroyed	52
	428	RT	$EuBr_2$-phase	enhanced	
KBr	459	200°C	Metastable phase	destroyed	
	428	200°C	$EuBr_2$-phase	enhanced	52
KCl	410	200°C	$EuCl_2$-phase	enhanced	
	440	200°C	Metastable phase	destroyed	52
	478	200°C	Metastable phase	destroyed	
RbBr	427	200°C	Eu-Br_2-phase	enhanced	
	440	200°C	Metastable phase	destroyed	54
	464	200°C	Metastable phase	destroyed	
RbBr	430	70°C	Suzuki-phase	destroyed	54
	450	---	---	generated	

Table I. Effects of X-irradiation on the europium precipitated phases in some alkali halides.

TABLE II

Host	Annealing Temperature in celcius degrees	Emission Band (nm)	Assignation	Effect on F-coloring relative to dipoles	Ref.
KBr	RT	423	Dipoles, dimers, etc.	Increases	55
		433	Suzuki		
	200	428	$EuBr_2$	Reduces	
		459	Metastable phase		
KI	RT	433	Dipoles, etc.	Increases	55
		438	Suzuki		
	270	421	EuI_2	Reduces	
		450	Metastable phase		
		470	Metastable phase		
RbBr	70	419	Dipoles, etc.	Reduces	55
		430	Suzuki		
	200	428	$EuBr_2$		
		440	Metastable phase	Reduces	
		464	Metastable phase		

Table II. F-coloring efficiency for different Eu^{2+}-second phase precipitates.

4. CONCLUSIONS

The data discussed above give a strong support to the models of Aguilar et al. and Comins and Carragher, where it is considered that the main traps for the radiation induced interstitial ions are the impurity vacancy dipole complexes and that the transition from the first to the second stage of F-coloring is not due to the exhaustion of the interstitial traps. Although these models do not take into account the possibili-

ty that the impurity ions change their valence state by irradiation it has been found experimentally that the linear relationship between the amount of first stage coloration and the square root of the total initial impurity concentration still holds. At present a series of theoretical and experimental investigations are being performed in our laboratory in order to corroborate this point as well as to extend the theory to include the effect of valence change of the doubly valent impurity ions and to determine if the theory still predicts a linear relationship between n_F and $\sqrt{C}$.

It has been also shown for the first time through the series of works carried out in our laboratory that the state of aggregation precipitation state of the impurity ion has a considerable influence on the F-coloring rate. Unfortunately, this fact has not been taken into account in a large number of previous works, and therefore some reserve must be put on their conclusions.

Finally, a lot of experimental evidence has been gathered to show that for heavily doped samples the radiation process enhances considerably the dipole aggregation rate.

REFERENCES

1. N.F. Mott and R.W. Gurney, Electronic Processes in Ionic Crystals, Oxford, London (1948).
2. J.H. Schulman and W.D. Compton, Color Centers in Solids, MacMillan, New York (1962).
3. R.E. Howard, S. Vosko and R. Smoluchowski, Phys. Rev., 122 (1961) 1406.
4. N. Itoh, J. Phys., 37 (1976) C7-27.
5. P.D. Townsend, J. Phys. C: Sol. St. Phys., 9 (1976) 1871.
6. N. Itoh, Cryst. Latt. Defects, 3 (1972) 115.
7. J.H. Crawford, Adv. Phys., 17 (1968) 93.
8. V.K. Jain, Phys. Stat. Sol. (b), 44 (1971) 11.
9. R.T. Williams, Semicond. and Insulat., 3 (1978) 251.
10. F. Agulló-López, F.J. López and F. Jaque, Cryst. Latt. Def. and Amorph. Mat., 9 (1982) 227.
11. M. Saidoh and P.D. Townsend, Rad. Eff., 27 (1975) 1.
12. N. Itoh, A.M. Stoneham and A.H. Harker, J. Phys. Soc. Japan, 49 (1980) 1364; J. Phys. C: Sol. St. Phys., 10 (1980) 4197.
13. N. Itoh and M. Saidoh, J. Phys., 34 (1973) C9-101.
14. J. Hoshi, M. Saidoh and N. Itoh, Cryst. Latt. Def., 6 (1975) 15.
15. F.J. López, J.M. Cabrera and F. Agulló-López, J. Phys. C: Sol. St. Phys., 12 (1979) 1221.

16. M. Aguilar, F. Jaque and F. Agulló-López, J. Phys., 41 (1980) C6-341.
17. J.D. Comins and B.O. Carragher, J. Phys., 41 (1980) 166.
18. W.A. Sibley and J.R. Russell, J. Appl. Phys., 36 (1965) 810.
19. M. Ikeya, N. Itoh, T. Okada and T. Suita, J. Phys. Soc. Japan, 21 (1966) 1304.
20. M. Ikeya, K. Kusao, T. Okada, N. Itoh and T. Suita, J. Phys. Soc. Japan, 20 (1965) 289.
21. N. Itoh and M. Ikeya, J. Phys. Soc. Japan, 22 (1967) 1170.
22. J.H. Crawford and C.M. Nelson, Phys. Rev. Lett., 5 (1960) 314.
23. W. Hayes and G.M. Nichols, Phys. Rev., 117 (1960) 993.
24. W. Hayes, J. Appl. Phys., S-33 (1962) 329.
25. J.N. Marat-Mendes and J.D. Comins, Cryst. Latt. Def., 6 (1975) 141.
26. J.N. Marat-Mendes and J.D. Comins, J. Phys., 37 (1976) C7-132.
27. J.N. Marat-Mendes and J.D. Comins, J. Phys. Chem. Sol., 38 (1977) 1003.
28. K.J. Kao and M.M. Perlman, Phys. Rev., B19 (1979) 1196.
29. R. Muccillo and J. Rolfe, Phys. Stat. Sol. (b), 61 (1974) 579.
30. M. Aguilar, F. Jaque and F. Agulló-López, Rad. Eff., 61 (1982) 215.
31. J.D. Comins and B.O. Carragher, Phys. Rev., B24 (1981) 283.
32. J. Hernández A., W.K. Cory and J. Rubio O., Japanese J. Appl. Phys., 18 (1979) 533.
33. J. Hernández A., H. Murrieta S., F. Jaque and J. Rubio O., Sol. St. Comm., 39 (1981) 1061.
34. J. Hernández A., W.K. Cory and J. Rubio O., J. Chem. Phys., 72 (1980) 198.
35. J. Hernández A., F.J. López, H. Murrieta S. and J. Rubio O., J. Phys. Soc. Japan, 50 (1981) 225.
36. J. Rubio O., M. Aguilar G., F.J. López, M. Galan, J. García-Solé and H. Murrieta S., J. Phys. C: Sol. St. Phys., 15 (1982) 6113.
37. F.J. López, H. Murrieta S., J. Hernández A. and J. Rubio O., Phys. Rev., B22 (1980) 6428.
38. M. Aguilar G., J. García-Solé, H. Murrieta S. and J. Rubio O., Phys. Rev., B26 (1982) 4507.
39. J. Rubio O., M.C. Flores, H. Murrieta S. and J. Hernández A., Phys. Rev., B26 (1982) 2199.
40. J. García M. J. Hernández A., H. Murrieta S. and J. Rubio O., Sol. St. Comm., 47 (1983) 515.
41. S. Ramos B., H. Murrieta S., M. Aguilar G. and J. Rubio O., Rad. Eff. Lett., 68 (1983) 173.
42. B. Kowalczyk and J.Z. Damm, Acta Phys. Polon., A49 (1976) 713.
43. J.L. Pascual and F. Agulló-López, Cryst. Latt. Def., 7 (1977) 161.
44. C. Medrano P., J. García-Solé, H. Murrieta S., J. Rubio O. and F. Agulló-López, Sol. St. Comm., 45 (1983) 775.
45. J.L. Pascual, J.M. Cabrera and F. Agulló-López, Sol. St. Comm., 19 (1976) 917.
46. J.L. Pascual, L. Arizmendi, F. Jaque and F. Agulló-López, J. Lumin., 17 (1978) 325.
47. E. Orozco M., A. Mendoza A., J. Soullard and J. Rubio O., Japanese J. Appl. Phys., 21 (1982) 249.
48. H. Murrieta S., F.J. López, J. García-Solé, M. Aguilar G. and J. Rubio O., J. Chem. Phys., 77 (1982) 189.
49. J. García-Solé, M. Aguilar G., F. Agulló-López, H. Murrieta S. and J.

Rubio O., Phys. Rev., B26 (1982) 3320.
50. J. Rubio O., H. Murrieta S., J. Hernández A. and F.J. López, Phys. Rev., B24 (1981) 4847.
51. M. Aguilar G., J. García-Solé, H. Murrieta S. and J. Rubio O., Rad. Eff. Lett., 68 (1982) 63.
52. M. Aguilar G., J. García-Solé, H. Murrieta S. and J. Rubio O., Rad. Eff., 77 (1983) 111.
53. F. Cussó, J. García-Solé, H. Murrieta S. and J. Rubio O., Cryst. Latt. Def. and Amorph. Mat. (in press).
54. C.C.R. Mediano P., Ph.D. Thesis, unpublished.
55. J.A. García M., Ph.D. Thesis, unpublished.